QUALITY BY DESIGN ENABLES FORMULATION DEVELOPMENT OF ZOLMITRIPTAN lOADED ETHOSOMAL INTRA-NASAL GEL FOR BRAIN TARGETING: IN VITRO AND EX VIVO EVALUATION

NAGADIVYA NERELLA*[ID], BAKSHI VASUDHA#[ID]

School of Pharmacy, Anurag University, Venkatapur, Ghatkesar Rd, Hyderabad, Telangana-500088, India
*Corresponding author: Nagadivya Nerella; Email: deanpharmacy@anurag.edu.in

ABSTRACT

Objective: Although zolmitriptan's 50% oral bioavailability and recurrence of migraine-associated disorders make it one of the most essential drugs for managing the illness, adverse effects linked to dosage are still a concern. A unique intra-nasal brain targeting strategy may significantly extend the drug's residence duration at the absorption site and resolve the current problems.

Methods: To effectively adjust the drug's residence via the intra-nasal route, the current study focuses on the development of zolmitriptan-loaded ethosomal gel with the help of soya lecithin, ethanol, poloxamer 407, and HPMC K100M utilizing the thin film hydration technique. The optimized formulation (F12) was completely characterized in terms of polydispersity index, vesicle size (nm), and entrapment efficiency (%). In vitro drug release at 24 h, stability study, and ex-vivo skin permeation pharmacodynamic studies were all evaluated.

Results: The ethosomal formulations were optimized using 3^2 Central Composite Design (CCD) about the observed responses, which comprised vesicle size, entrapment efficiency, and percent drug release after 24 h, all included in this study. The optimal size range and zeta potential for the F12 formulation were determined to be 110.23 nm and-35.69, respectively. The generated drug-loaded ethosomal gel was spherical with a consistent size distribution and particle size. Morphological studies showed that Scanning Electron Microscope (SEM) was utilized to better study spherical multilamellar vesicles. The optimized ethosomal gel of zolmitriptan was determined to meet the stability criterion, as the Critical Quality Attributes (CQAs) did not vary significantly during the study period.

Conclusion: For all formulations, the F12 batch showed vesicle size (110.23 nm), entrapment efficiency (82.02%), and drug release percentage of 89.26% at 24 h.

Keywords: Ex vivo permeation, Intranasal administration, Zeta potential, Vesicle size, Film hydration, Central composite design

INTRODUCTION

The primary symptom of a migraine is pulsatile headaches, which are caused by a number of reasons. After which comes phonophobia, photophobia, vomiting, nausea, and anorexia, all of which are made worse by physical exertion [1]. A prevalent ailment, migraines place a significant health cost on sufferers as well as on society, resulting in missed work and productivity losses that have an adverse financial impact. Zolmitriptan selectively acts on serotonin (5HT1B/1D) receptors, zolmitriptan (4S-4-({3-[2-(dimethylammino) ethyl]-1H-indol-5-yl} methyl-1,3-oxazolidin-2-one) is a second generation triptan that is very effective and well-tolerated in treating acute migraine associated with menses and migraine with aura [2]. Additionally useful in treating acute cluster headaches [3, 4], Zolmitriptan (ZOL) narrows brain blood vessels by activating serotonin receptors, a naturally occurring brain chemical. By activating serotonin receptors, zolmitriptan mimics this effect of serotonin and inhibits peripheral blood vessel dilatation and cranial vascular inflammation. Zolmitriptan has a dependable patient acceptance rate, but its frequent dosage requirements and related side effects restrict its utilization. In order to decrease related adverse effects, a new dosage form for brain-targeted, prolonged, and continuous zolmitriptan administration must be developed. As of right now, the market offers selected pure drug formulations in tablet, nasal spray, and orodispersible tablet dosage forms [5, 6].

However, since migraine sufferers experience nausea and stomach issues, the usage of these dose forms is restricted [7]. To get over these restrictions, a nano-formulation that targets the brain and delivers a prolonged release of medication is required. A method that may be used to circumvent the blood-brain barrier and operate as a medication carrier is the nano-ethosomal drug delivery system, which is facilitated via the olfactory lobes route [8, 9]. We have presented our study effort here, using 3^2 central composite design to construct and improve drug ethosomes. Using HPMC K100M as a mucoadhesive agent and poloxamer 407 as a thermo-reversible gelling agent, optimized ethosomes were assessed and subsequently integrated into thermo-sensitive gel form.

MATERIALS AND METHODS

Materials

The pure drug was obtained as a free sample from M/s Cipla ltd., Mumbai, India; phospholipid i. e. soya lecithin (99% pure), poloxamer 407, HPMC K100M, was purchased from Sigma Aldrich. Ethanol, methanol, propylene glycol and other solvents were procured from Merck ltd., India. All other chemicals and reagents were obtained from local supplier and of analytical grade.

Methods

Preformulation studies

Solubility studies

Acetone, ethanol, Dimethylsulfoxide (DMSO), distilled water, phosphate buffers 6.8 and 7.4, 0.1N HCl, methanol, acetonitrile, Dimethylformamide (DMF), Polyethylene Glycol (PEG)-200, and 400 were all used to test the drug's solubility. Each solvent was mixed with a suitable amount of the ZOL, and the mixture was shaken for 72 h in a mechanical shaker (Model: Reciprocating (Horizontal) 50111001 Rivotek, Riviera Glass Pvt. ltd. in a water bath at a temperature maintained at 37±0.5 ℃. The drug's complete solubilisation in the vials was regularly checked. To get rid of any drug that were intractable or immiscible, all mixes were permitted to be put into centrifuge tubes [10].

UV estimation of Zolmitriptan (ZOL) in 0.1N HCl

To create a stock solution of 1000g/ml (ppm), 100 mg of drug was meticulously weighed and completely dissolved in 10 ml of 0.1N

HCl. The volume was then raised to the required mark of 100 ml. Next, a 100g/ml (ppm) concentrated solution was obtained by diluting 10 ml of the standard working solution with 0.1N HCl (Model no. UV-visible spectrophotometer UV-1800 lab India ltd., Mumbai, India). Further examined these solutions between 200 and 400 nm in wavelength. The accompanying UV spectra curve was recorded at the wavelength where the greatest absorbance was indicated for further dilutions of concentrated solutions containing 10, 50, 100, 150, 200, 250 µg/ml. It was discovered that the maximum wavelength of λ_{max} was 283 nm. Following serial dilutions, a calibration curve was created with a R^2 value of 0.9968 at λ_{max} 283 nm, ranging from 10 to 250 µg/ml [11].

Fourier-Transform Infrared Spectroscopy (FT-IR)

The drug zolmitriptan was shown to have physical interactions using FT-IR spectrometry (Shimadzu Analytical, India, Pvt. ltd., Model No. Shimadzu IR affinity-1., ltd). Potassium bromide was used to create the FT-IR spectra of zolmitriptan and physical combinations (PM) with soy-lecithin and poloxamer 407. In order to assess the drug-excipient interaction, transmittance from 4000 to 400 cm^{-1} was computed. To determine if there was any interaction between zolmitriptan and the other excipients, peak matching was used [12].

Differential Scanning Calorimetry (DSC)

In order to investigate the drug's compatibility with the phospholipid, (Model No. DSC (Differential Scanning Calorimetry, SHIMADZU DSC-60). ltd) was used. In aluminium pans, dried nitrogen was used as the effluent gas to warm each specimen (10 mg). The physical combinations of poloxamer 407, soy lecithin, and zolmitriptan (ZOL) were ascertained using DSC thermogram analysis [13].

Quality Target Product Profile (QTPP) and Critical Quality Attributes (CQAs)

A Quality-Based Design (QbD) driven approach was used in the medication formulation development process. In order to formulate the dosage with enhanced performance and therapeutic advantages, a Quality Target Product Profile (QTPP) was first established. As shown in table 1, basic consideration was given to dosage type (sustained), dosage form (Intra-nasal gel), and drug release. Essential CQAs were identified as quality characteristics of flexible vesicles, including both formulation and physical attributes, in order to fulfil the requirements of defined QTPP. The most important quality criteria that were found to be responsible for the product's performance were the cumulative drug release after 24 h, vesicle size and the percentage of entrapment efficiency [14].

Table 1: Quality target product profile (QTPPs) and critical quality attributes (CQAs) for developing zolmitriptan loaded intra-nasal ethosomal gel

QTTPs	Target	CQAs	Predetermined target	Justification
Dosage type	Sustained release dosage forms	Cumulative drug release at 24h (%)	≥ 80%-95%	Sustained release of drug is the objective of the study and is important for better drug absorption.
Dosage form	Intra-nasal Ethosomal gel	Vesicle size (nm)	100-200 nm	Highly critical factor as its role in permeation and retention of bio-actives in the intra-nasal route.
Drug release	Higher entrapment	Entrapment efficiency (%)	≥ 80%-95%	Higher entrapment is highly critical and important for better drug loading and drug release.

Formulation of zolmitriptan-loaded ethosomal gel

Using varying quantities of phospholipid (soya lecithin) (20–40 mg/ml), ethanol (15, 25, and 35%) as a harvesting solvent, propylene glycol (10% v/v), drug (20 mg), and water (qs 100% w/w), drug-loaded ethosomal gel were made using the traditional thin film hydration process. Phospholipid was dissolved in a 250 ml round-bottom flask containing a 2:1 v/v ratio of chloroform to methanol. Vacuum was initiated after 30 s to extract the solvent entirely. The aforementioned mixture was kept constant by heating above the lipid transition temperature (55±2 °C) at 60 rpm until full evaporation, provided the condenser be refrigerated for effective removal of the organic solvent [15]. After that, the film was hydrated for 30 min at a temperature of 55±2 °C, above the lipid transition temperature, using medication and propylene glycol mixed in ethanolic solution. Lipid was fully swelled to produce vesicular dispersion, which was then maintained at room temperature for two h. After that, the obtained dispersion was exposed to three cycles of 15 min each (15 s on/off cycle) of probe sonication (Rivotek

Ultrasonic Sonicator, Mumbai, India) for a total of 45 min. After then, the formulation was refrigerated for further characterization [16].

Analysis of risk assessment

Risk assessment studies were used to examine several quality aspects related to ethosomes. The Ishikawa fishbone diagram for ethosomes creation was used in the process. The primary goal is to examine the cause-and-effect connection between a number of process parameters (PPs) and Critical Material Characteristics (CMAs), as well as the anticipated impact of these on the ethosomes Critical Quality Attributes (CQAs). Failure Mode and Effect Analysis (FMEA) was used to identify the critical risk variables that had the greatest impact on the chosen CQAs [17, 18] The risk priority number (RPN) was determined by assigning rank order scores (ranging from 1 to 10) as depicted in table 2 to the material and process parameters attributes based on severity (S), occurrence (O), and detectability (D) through an extensive literature survey, prior knowledge, and brainstorming exercises.

Table 2: Factor analysis of materials and process variables using FMEA (Failure mode and effects analysis) tool during the preparation of zolmitriptan-loaded intra-nasal ethosomal gel

Process parameters	Risk priority number (RPN)	Severity (S)	Occurrence (O)	Detectability (D)
Types of phospholipids	294	7	6	7
Concentration of phospholipid (Soya-lecithin) (mg/ml)	280	8	5	7
Type of aqueous phase	36	3	4	3
Volume of aqueous phase (ml)	30	5	3	2
Concentration of ethanol (%) v/v	294	7	6	7
Stirring speed (rpm)	24	4	2	4
Stirring speed	252	6	6	7
Stirring time (min)	280	8	7	5
Stirring type	288	8	6	6
Sonication speed per time	336	8	6	7

Using Taguchi orthogonal array (OA design) for preliminary screening

To determine the most significant element or factors preventing the CQAs, an initial evaluation was carried out using a Taguchi design consisting of seven components and two tiers as shown in table 3. Eight different formulations for the Taguchi design of the experiment matrix were created and constructed, along with an assessment of the CQAs that were given. To determine each aspect's overall importance, an ANOVA was used as shown in table 4. In order to determine the crucial components, the p-value was finally actualized [19].

Table 3: Design matrix for the influential factors screening as per taguchi design, along with the experimental results of selected CQAs

Runs	Amount of zolmitriptan used (mg)	Coded factors and its low and high levels							Cumulative drug release at 24h (%)	Vesicle size (nm)	Entrapment efficiency (%)
		A	B	C	D	E	F	G			
1	20	1	2	2	1	1	2	2	66.85	259.45	66.98
2	20	2	2	1	2	1	1	2	39.23	435.46	22.36
3	20	2	1	2	1	2	1	2	47.45	365.36	63.54
4	20	1	1	1	2	2	2	2	87.23	202.9	86.54
5	20	2	1	2	2	1	2	1	50.36	315.23	65.02
6	20	1	1	1	1	1	1	1	79.58	232.56	75.98
7	20	2	2	1	1	2	2	1	40.23	385.22	30.69
8	20	1	2	2	2	2	1	1	58.34	295.47	59.36
Factors		Codes		Low level (1)			High level (2)				
Types of phospholipids (mg)		A		5			10				
Concentration of phospholipid (Soya-lecithin) (mg/ml)		B		10			20				
Concentration of ethanol (%) v/v		C		5			15				
Stirring speed (rpm)		D		1000			2000				
Stirring time (Minute)		E		30			60				
Stirring type		F		Mechanical			Magnetic				
Sonication speed per time (Hz/Minute)		G		1000/10			2000/20				

Table 4: Summary of ANOVA for factor screening and its significance as per Taguchi design

Factors	p-values of obtained from screened responses		
	Cumulative drug release at 24h (%)	Vesicle size (nm)	Entrapment efficiency (%)
Types of phospholipids (mg)	0.0058*	0.0002*	0.0078*
Concentration of phospholipid (Soya-lecithin) (mg/ml)	0.0111*	0.0006*	0.0134*
Concentration of ethanol (% v/v)	0.0287*	>0.1000	0.0269*
Stirring speed (rpm)	>0.1000	>0.1000	0.1112
Stirring time (Minute)	0.2307	0.0834	>0.1000
Stirring type	0.0333*	0.0015*	0.0323*
Sonication speed per time (Hz/Minute)	0.0544	0.0320*	0.0544

*Significant values, i. e., less than α value (0.05)

Table 5: Different formulation composition of zolmitriptan loaded intra-nasal ethosomal gel of obtained thirteen experimental runs as per CCD along with the obtained CQAs responses

Run	Amount of zolmitriptan used (mg)	Factor 1 (X1) A: Concentration of soya-lecithin (mg/ml)	Factor 2 (X2) B: Concentration of ethanol (% v/v)	Response (Y1) Cumulative drug release at 24h (%)	Response (Y2) Vesicle size (nm)	Response (Y3) Entrapment efficiency (%)
1	20	0	0	64.26	196.25	60.89
2	20	-1	0	29.65	322.69	24.3
3	20	0	-1	36.25	301.55	30.77
4	20	-1	1	30.22	322.58	29.36
5	20	1	0	80.22	129.36	75.22
6	20	0	0	59.68	212.07	55.04
7	20	-1	-1	20.69	355.29	16.92
8	20	0	0	52.02	224.88	50.36
9	20	0	0	49.66	255.02	47.07
10	20	0	1	75.23	155.02	66.2
11	20	1	-1	39.22	296.78	36.97
12	20	**1**	**1**	**89.26**	**110.23**	**82.02**
13	20	0	0	42.22	268.33	40.12
Independent Variables				Coded and actual levels		
				Low (−1)	Medium (0)	High (+1)
A: Concentration of soya-lecithin (mg/ml)				20	30	40
B: Concentration of ethanol (% v/v)				15	25	35

Statistical optimization of ethosomal intranasal gel of zolmitriptan by central composite design

To maximize the many important material properties impacting the response variables, or critical quality attributes, a two-factor, three-level central composite design was used as shown in table 5. Three distinct degrees of variation were observed in the concentrations of ethanol (X2) and soy lecithin (X1), which were identified as separate key material qualities. Three dependent quality attributes were evaluated: vesicle size (Y3), % entrapment efficiency (Y2), and % drug release (Y1). Thirteen batches in all were made, with four

centre points for each block. Design expert software (Design Expert 13, Stat-Ease, Minneapolis, MN) was fitted with the acquired data. To build an understanding of the connection between the variables and their interaction, response surface studies were performed and contour plots and three-dimensional (3D) response surface plots were generated. Second-order polynomial models were created and put into a multiple linear regression model in order to determine the impact of various CMAs on CQAs. Design validation was carried out using analysis of variance (ANOVA) [20]. Quality attribute constraints were established at goal levels, and potential formulation composition was ascertained via the use of Design Expert software's checkpoint analysis and desirability technique. A numerical optimization process using the desirability function was used to choose the best formulation [21, 22].

Characterization of drug-loaded ethosomes

Entrapment efficiency (%)

When the deformable vesicles, or ethosomes, were separated from the solution using the centrifugation procedure, the drug entrapment effectiveness of the ethosomes was recorded. The estimate process included extracting 10 milliliters of ZOL-loaded ethosomal dispersions and centrifuging them for one hour at-4 °C for 50,000 rpm using a cooling centrifuge (Model: Eltec lab RC 4815). The unentrapped free medication is partially removed by the centrifugation dialysis procedure [23]. The supernatant liquid was collected and subjected to UV spectrophotometric analysis at a wavelength of 283 nm (UV 1800, Shimadzu, Japan) to determine the presence of free medication (zolmitriptan), calculated, as shown in Eq. (1);

$$\% \text{ Entrapment efficiency} = \frac{\text{Total drug quantity} - \text{Quantity of free drug}}{\text{Quantity of total drug}} \times 100 \dots [\text{Eq. 1}]$$

Vesicle size, polydispersity index (PDI) and zeta potential determination

The Malvern equipment (Model: Malvern ZETASIZER NANO ZS Malvern ZEN3600 RED) equipped with (PCS) photon correlation spectroscopy was used to measure the vesicle size. This spectroscopy was assumed to estimate and evaluate the particle size and zeta potential. The polydispersity index was computed and a size distribution was provided. Zeta potential levels have a significant impact on the homogeneity within the ethosomal dispersion [24-26].

Scanning electron microscopy (SEM)

The improved formulation's morphologic analysis was carried out using a TEM (JEOL JEM1230, Tokyo, Japan) running at an 80 kV accelerating voltage. A single droplet of dispersion was applied to the surface of a copper grid covered with carbon and allowed to stick to the carbon substrate for a minute. Any remaining dispersion was then eliminated using a filter paper tip [27].

Powder X-ray diffraction (p-XRD)

For the diffraction experiments, a powder X-ray diffractometer (Model: Rigaku, Japan, Smart lab 9 kW) was used. The samples were scanned for powder XRD after being exposed to nickel-filtered CuKa radiation (40 kV, 30 mA). Plotting the data as peak height (intensity) vs time (h) was done using ZOL pure medication and improved ethosomal formulation [28].

In vitro release studies of drug-loaded ethosomal gel

The *in vitro* release from drug-loaded ethosomal gel formulations was investigated using the USP dissolution test device (Pharma Test dissolution Tester, Germany). In this *in vitro* drug release investigation, the dialysis bag diffusion technique (Himedia; Dialysis Membrane-60; Average flat width: 25.27 mm, Average diameter: 15.9 mm with 10000 kDa–12000 KDa with 5 ml capacity) was utilized for drug-loaded ethosomal gel, which is equal to 2 mg drug. Five millilitres of each formulation were put into a dialysis membrane, sealed, and submerged in 150 millilitres of 0.1N HCl under sink conditions for the first 2h. After that, it was submerged for 24 h in a 7.4 pH phosphate buffer solution. The system was kept at 37 °C with 500 rpm of continuous magnetic stirring. After that, samples (2 ml) were taken out at pre-arranged intervals of time (0.5,

1, 2, 3, 4, 5, 6, 7, 8, 24 h) and replaced with 0.1 N HCl and pH 7.4 phosphate buffer to sustain sink conditions, and spectrophotometrically measured at λ_{max} 283 nm with a blank of 0.1 N HCl for 2 h and pH 7.4 phosphate buffer for 24 h separately. The findings were reported as means (n = 3±SD) [29].

Ex vivo skin permeation studies

Using removed goat nasal mucosa, the goat nose was collected from the local abattoir within 15 min of the goat being slaughtered. After removing the cartilage and blood, the isolated nasal mucosa was washed and preserved in newly made phosphate-buffered saline (pH 6.4). Six systems of Franz diffusion cells with thermostat capabilities were used for the experiment. Nasal tissues were chosen for the investigation and immersed for one hour in the diffusion medium (Phosphate-buffered saline, or PBS; pH 7.4). While the receptor compartments were filled with phosphate buffer pH 7.4, the donor compartment of Franz diffusion cells was covered with nasal tissues with an operational permeation area of 2×2 cm^2. The investigation was carried out with an ideal stirring speed of 34±1 °C [30-32]. Concurrently, 200 μl of drug-loaded ethosomal gel, or 2.5 mg, was put into the donor compartment. Samples (0.5 ml) were taken out of the receptor compartment and replaced with new buffer for a period of 24 h at the predetermined intervals of 1, 2, 4, 6, 8, 12, and 24 h. At λ_{max}283 nm, the samples were examined using a UV spectrophotometer. Under steady-state circumstances, the effective permeability coefficient (mm/s) across the goat nasal mucosa was computed using the following Eq. (2);

$$\text{Permeability coefficient} = \left(\frac{dc}{dt}\right) ss \times \frac{V}{A \, Cd} \dots \dots [\text{Eq. 2}]$$

Where (dc/dt) ss (μg ml^{-1} s^{-1}) is the change of concentration under steady state; A (cm^2) is the permeation area; V (ml) is the volume of the receiver compartment; and Cd (μg ml^{-1}) is the initial donor concentration.

Stability analysis

Stability experiments were conducted on optimized ethosomal formulation in order to assess the impact of various storage conditions. For the duration of the investigation, the formulations were maintained at room temperature (25±2 °C/60±5% RH) and refrigerated condition (4±2 °C). Physical and chemical stability of the formulation were assessed at intervals of 0, 1, 3, and 6 months. Analysing drug release at 24 h, vesicle size, and formulation entrapment effectiveness percentage allowed for the study of physical stability [33].

RESULTS AND DISCUSSION

Solubility study analysis

The drug solubility in several solvents is shown in fig. 1a. The solubility of drug is maximum in 0.1N HCl (4932.65±2.2 μg/ml) and ethanol (5036.25 ±2.1 μg/ml), with no discernible variation between the two [34].

Spectrophotometric estimation of pure drug in 0.1N HCl

After analysing solvent interference, the drug was measured spectrophotometrically against 0.1N HCl to construct a calibration curve for pure drug at λ_{max} 283 nm (fig. 1b). Fig. 1c displays the correlation coefficient (R^2= 0.9968) and linear correlation for drug ranging from 10 to 250 μg/ml [34].

FT-IR studies

Fig. 2 (a-e) showing the comparison of the FT-IR spectra of the ethosomal formulation of F12 with the pure drug. The bands resulting from N-H stretching at 3346.64 cm^{-1}, C=O stretching at 1738.90 cm^{-1}, and C=C stretching at 1479.47 cm^{-1} are present in the pure drug. Similar functional groups that display bands as a consequence of N-H stretching at 3344.87 cm^{-1}, C=O stretching at 1725.90 cm^{-1}, and C=C stretching at 1649.49 cm^{-1} were also present in the improved formulation F12. Therefore, there is compatibility between the pure drug and the excipients [35].
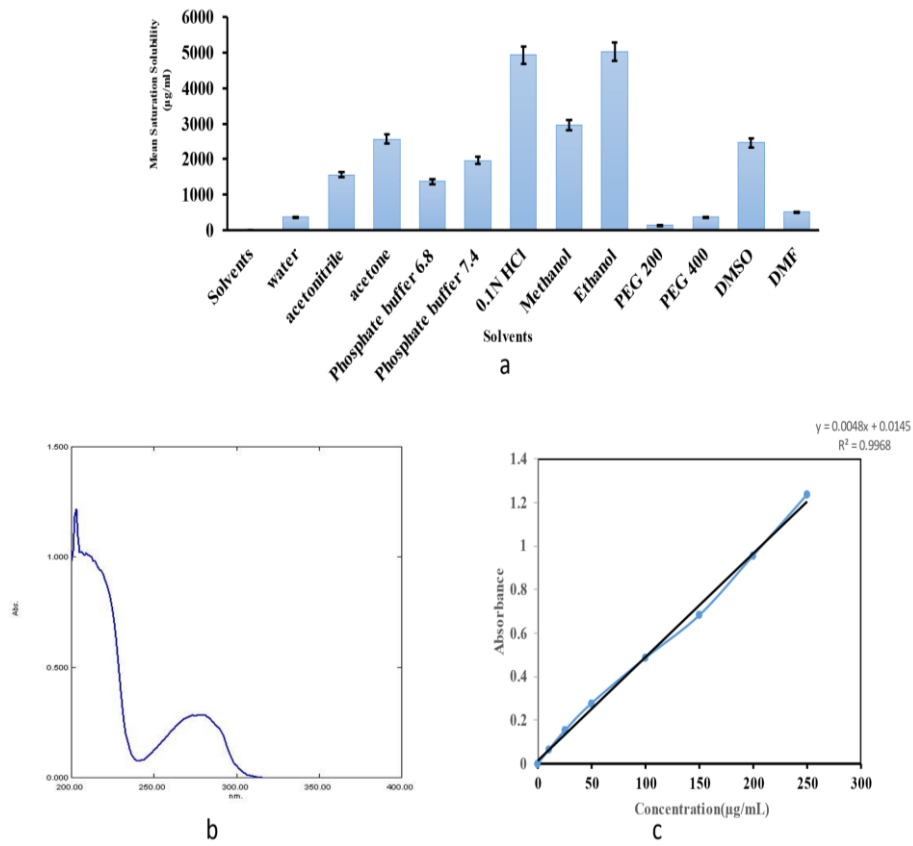
Fig. 1: The mean saturation solubility bar graph of pure drug (zolmitriptan) in different solvents (a), absorption spectra of pure drug in 0.1N HCl at λ_{max} 283 nm (b), and calibration curve of pure drug (c) in 0.1N HCl at λ_{max} 283 nm, all data showed as mean±SD (n=3); where n is the number of observations in fig. 1a
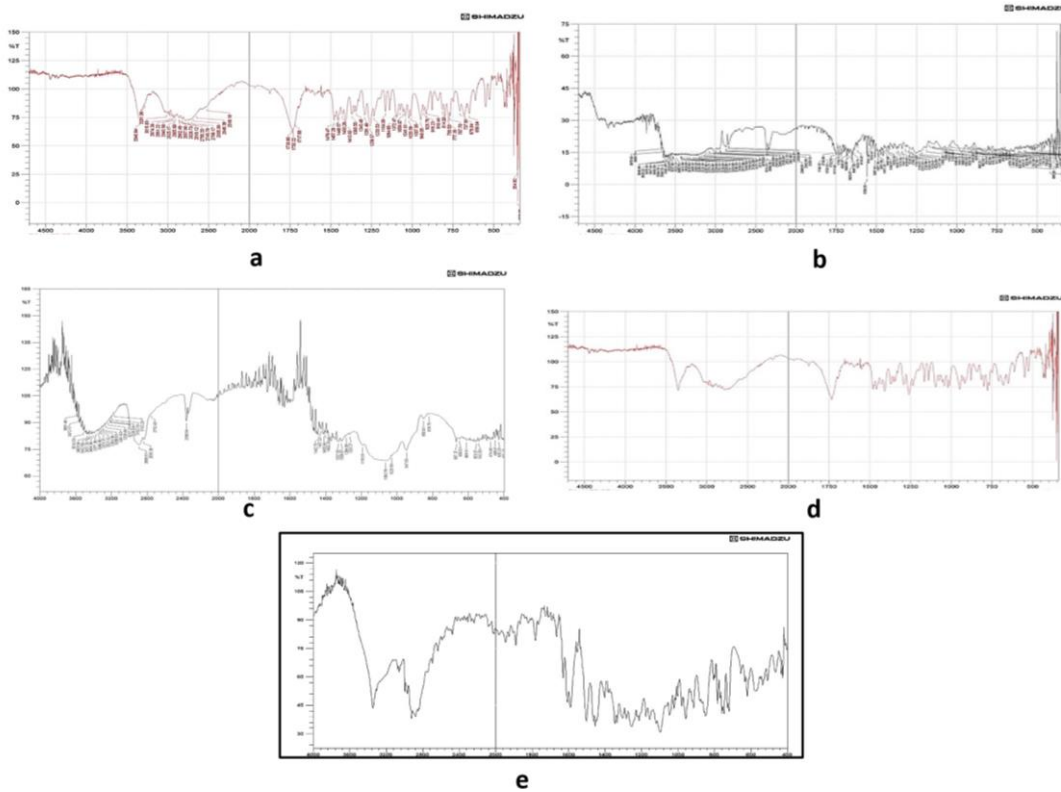

Fig. 2: FT-IR spectra of zolmitriptan (a), soy-lecithin (b), HMPC K100M (c), physical mixture (PM) of pure drug with soy-lecithin and HMPC K100M (d), optimized ethosomal F12 formulation (e)

DSC studies

Fig. 3 (a-d) is a representation of DSC thermograms. The pure drug showed a clear endothermic peak at 141.18 °C, with corresponding onset and end set temperatures of 136.65 °C and 145.66 °C. In addition, the lyophilized formulation (F4) had a pronounced endothermic peak at 120.09 °C, with start and end set temperatures ranging from 113.29 to 125.9 °C. These results suggested that the drug and the other ingredients in the formulation above did not interact. Additionally, it shows that the ethosomal formulation (F12) has less crystallinity because of the weaker peak [36].
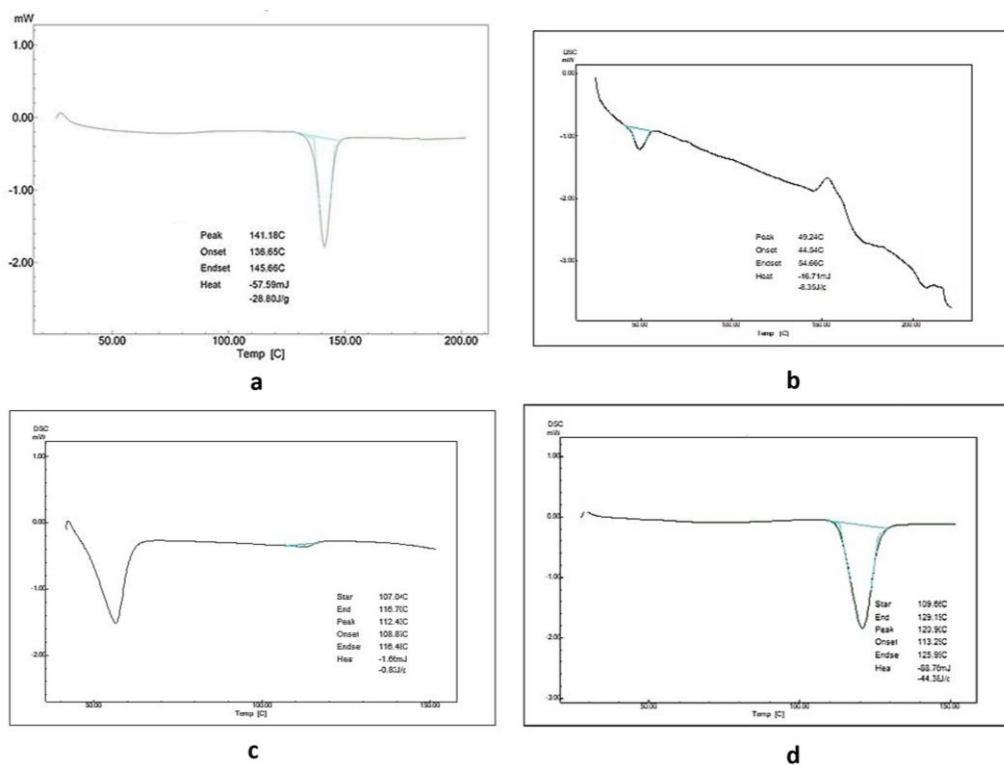
Fig. 3: DSC thermograph of zolmitriptan (a), soy-lecithin (b), pure drug with soy-lecithin (c), optimized ethosomal F12 formulation (d)
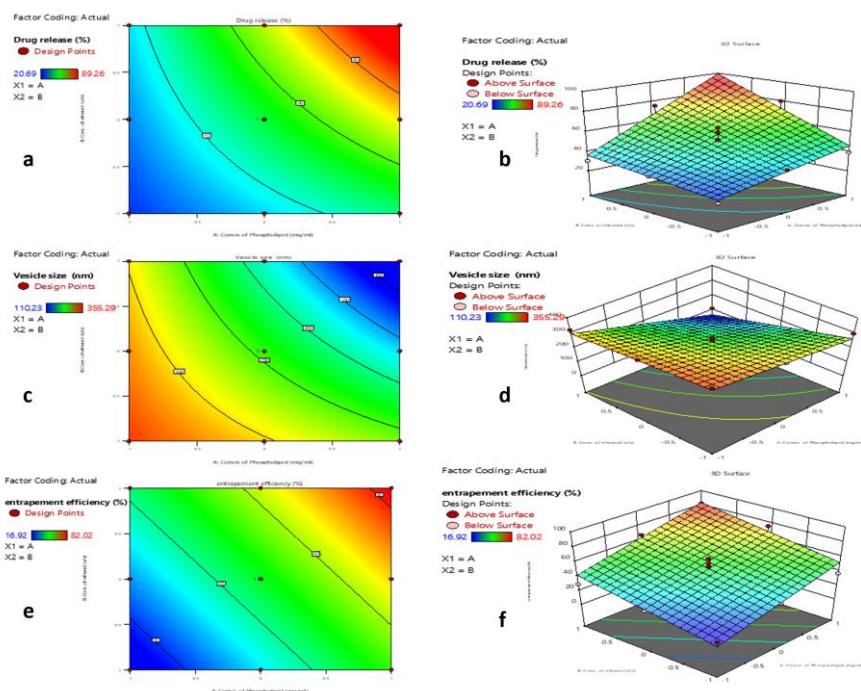

Fig. 4: The contour plots (2D) and response surface plots (3D) of selected independent factors on selected dependant factors, cumulative % drug release at 24 h (a and b), vesicle size (c and d), and % entrapment efficiency (e and f), 2D and 3D response surfaces' interpretations

Statistical optimization by central composite design and response surface methodology

The ANOVA and lack of fit were also statistically tested on the model. A substantial p-value was found in the model terms (0.05), and the model was best suited as shown in table 6 and table 7. Outlines of the central composite model was determined by fitting it into an appropriate mathematical model, particularly a quadratic model, demonstrating interaction effects among the variables. The direct effect of selected independent factors, such as concentration of soya lecithin (A) and concentration of ethanol (B), with additional impact of these individual variables on observed responses (% drug release 24h, vesicle size in nm, and % entrapment efficiency). Moreover, trapping and drug release were significantly impacted by the soy lecithin content. According to published research, there is a positive correlation between the concentration of soy lecithin and the percentage entrapment efficiency. Drugs that are lipophilic have a tendency to dissolve more readily in lipid, which increases the effectiveness of entrapment [37]. Since zolmitriptan is lipophilic by nature, it dissolves easily in soy lecithin, indicating that soy lecithin concentration is the primary factor influencing entrapment efficiency [38]. The optimal formulation, Formulation 12, demonstrated the maximum percentage of entrapment and drug release with the desired vesicle size as shown in the 2D and 3D plots of fig. 4 (a-f).

Meanwhile, ethanol simultaneously plays a synergistic role in solubilizing lipophilic drugs, which subsequently enhances entrapment efficiency and drug release of the ethosomal vesicles [39].

The mathematical model elucidates the quadratic polynomial equations for individual responses as shown in Eq. (3 to 5);

Cumulative % drug release 24h

$$= +51.43 + 21.36 * A + 16.42 * B + 10.13 * AB \dots (3)$$

$$\text{Vesicle size (nm)} = +242.31 - 77.37 * A - 60.97 * B - 38.46 * AB \dots (4)$$

$$\text{Entrapment efficiency (\%)} = +47.33 + 20.60 * A + 15.49 * B \dots (5)$$

Effect of the factor on cumulative drug release (%) after 24 h

Fig. 4 (a and b) show the contour plot and 3D plot for the CQAs cumulative drug release 24 h. Comparing these formulations, trial run 12 seemed to have the greatest percentage of drug release, at 8926%. Run 7 shows a minimum value of 20.69%, indicating more than 80% drug release in 24 h. Based on the simulations, this reddish-yellow zone is predicted to be prevalent at a high level (+1) of soya lecithin concentration and a high level (+1) of ethanol concentration. However, the blue zone with the least amount of drug release was shown to be prevalent at low levels (-1) of soy lecithin and ethanol concentration [39].

Table 6: Summary of ANOVA for different factors and its significance with respect to quadratic model

Source	Cumulative drug release at 24h (%)		Vesicle size (nm)		Entrapment efficiency (%)	
	F-value	p-value	F-value	p-value	F-value	p-value
Model	5.28	0.0250*	10.05	0.0043*	4.44	0.0384*
A: Concentration of soya-lecithin (mg/ml)	8.69	0.0214*	10.15	0.0154*	9.91	0.0162*
B: Concentration of ethanol (% v/v)	1.66	0.2390	3.83	0.0912	1.20	0.3100
AB	1.16	0.3173	4.91	0.0623	1.60	0.2460
A^2	11.39	0.0118*	28.07	0.0011*	8.01	0.0254*
B^2	0.1995	0.6686	0.1131	0.7465	0.0021*	0.9650
Lack of fit	18.69	0.0081*	6.70	0.0487*	4.50	0.0900

*Significant levels, i. e., less than α value (0.05)

Table 7: Summary of design of experiment with various parameters fitting to quadratic model

Responses	Cumulative drug release at 24h (%)	Vesicle size (nm)	Entrapment efficiency (%)
R^2	0.7905	0.8778	0.7603
Adjusted R^2	0.6408	0.7874	0.5860
Predicted R^2	0.5308	0.0678	-0.5011
Adeq Precision	5.5530	8.138	5.597
Std. Dev.	14.79	110.07	5.99

R^2; Correlation coefficient; Std. Dev; Standard deviation

Effect of the factor on vesicle size (nm)

Fig. 4(c and d) depict the contour and 3D plots of CQA vesicle size. A comparison of these formulations found that trial run 12 appeared to have the smallest vesicle size, measuring 110.23 nm. Run 7 has the greatest vesicle size at 355.29 nm. This is the dark blue zone, which denotes the smallest vesicle size and is expected to be present at high levels (+1) of soy lecithin and (+1) of ethanol concentration. However, the light red zone had the highest vesicle size, which was prominent at low soy lecithin and ethanol concentrations (-1) [39].

Effect of the factor on % entrapment efficiency

Fig. 4(e and f) depict the contour and 3D plots of the CQA% entrapment efficiency. A comparison of these algorithms revealed that trial run 12 appeared to have the highest rate of entrapment, at 82.02%. The dark reddish zone, which is expected to be present at a high level (+1) of soy lecithin concentration and a high level (+1) of ethanol concentration, has the maximum entrapment, while run

number seven has the lowest entrapment, at 16.92%. However, the presence of the light blue zone with the least amount of entrapment was seen at low concentrations (-1) of soy lecithin and ethanol [39].

Analyses overlay plots to establish the design space

The optimised dug-loaded ethosomal gel, depicted as an overlay plot in the figure, was made using the central composite design and contained 20 mg drug, 40 mg/ml soy lecithin, and 35% v/v ethanol concentration. Table 8 provides a summary of the optimisation procedure, as well as experimental and forecasted values for the optimised formulation's responses. Fig. 5 depicts the region where adjusting the concentrations of independent factors can maximise the results of dependent variables. The region depicted in the graph contains numerous passes that provide the ideal factor values to ensure the feasibility of each operational constraint simultaneously. The overlay plot allows you to inspect process or formulation constraints [39].

Table 8: Constraints for the process of optimization of zolmitriptan loaded intra-nasal ethosomal gel using design of experiment (DoE)

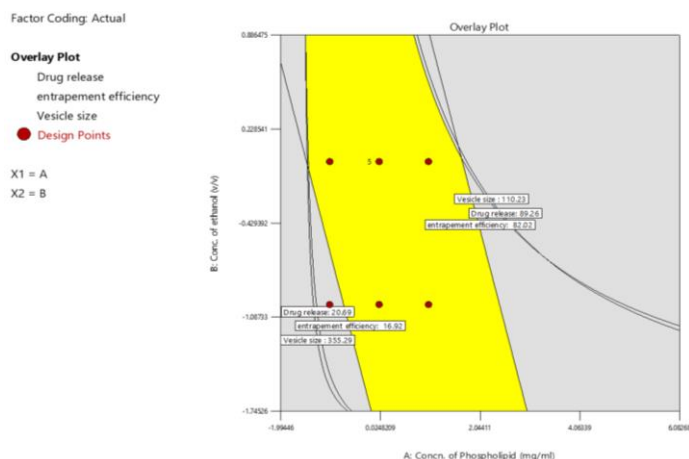| Optimized run-12 responses	Predicted mean	Observed	Std deviation	n	SE pred	95% PI low	95% PI high
Cumulative drug release at 24h (%)	99.3384	89.26	8.36988	1	10.7847	74.9418	123.735
Vesicle size (nm)	65.5215	110.23	33.3611	1	42.9861	-31.7198	162.763
Entrapment efficiency (%)	83.4178	82.02	9.02824	1	10.7214	59.529	107.307

Two-sided confidence = 95%

Fig. 5: Overlay plot of factors and its associated responses within the design space through graphical optimization

Table 9: Characterization data of 13 formulations of zolmitriptan-loaded intra-nasal ethosomal gel

Formulation code	Zeta potential (mv)	Polydispersity index	Vesicle size (nm)	Entrapment efficiency (%)
F1	0.190±0.67	-20.76±0.72	196.25±0.51	60.89±0.66
F2	0.196±0.61	-20.03±0.77	322.69±0.55	24.3±0.63
F3	0.201±0.62	-19.99±0.72	301.55±0.57	30.77±0.69
F4	0.210±0.66	-20.99±0.75	322.58±0.59	29.36±0.59
F5	0.342±0.60	-20.85±0.73	129.36±0.52	75.22±0.57
F6	0.333±0.62	-20.19±0.71	212.07±0.55	55.04±0.68
F7	0.207±0.59	-19.99±0.77	355.29±0.57	16.92±0.66
F8	0.386±0.57	-10.78±0.75	224.88±0.53	50.36±0.71
F9	0.203±0.66	-18.76±0.77	255.02±0.50	47.07±0.77
F10	0.370±0.61	-21.03±0.72	155.02±0.54	66.2±0.73
F11	0.291±0.64	-10.09±0.74	296.78±0.52	36.97±0.72
F12	0.391±0.68	-21.05±0.74	110.23±0.59	82.02±0.75
F13	0.205±0.67	-20.01±0.79	268.33±0.53	40.12±0.77

All data showed as mean±SD (n=3); where n is the number of observations

Vesicle size, polydispersity index (PDI) and zeta potential

The zeta-sizer instrument analysed the particle size of all formulations. It was found that some formulations showed a larger particle size. The optimized size range for the F12 formulation was found to be (110.23 nm), i.e., for run 12 (fig. 6a). The developed drug-loaded ethosomal gels were spherical with uniform size distribution and particle size. The zeta potential results for the respective formulation were (-35.69) for run 12 (fig. 6b). Table 9, exhibits the obtained values for all the 13 formulations on the different characterization parameters and fig. 7(a-d) represents the bar diagrams for the reported values [39].
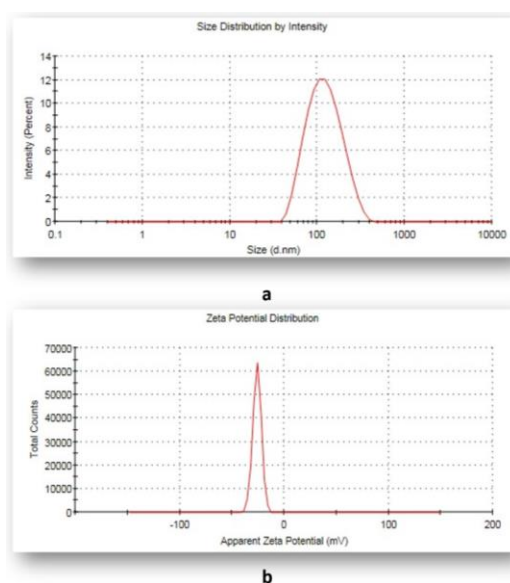

Fig. 6: Image showed particle size distribution by intensity (a) and zeta potential distribution curve of optimized ethosomal F12 formulation
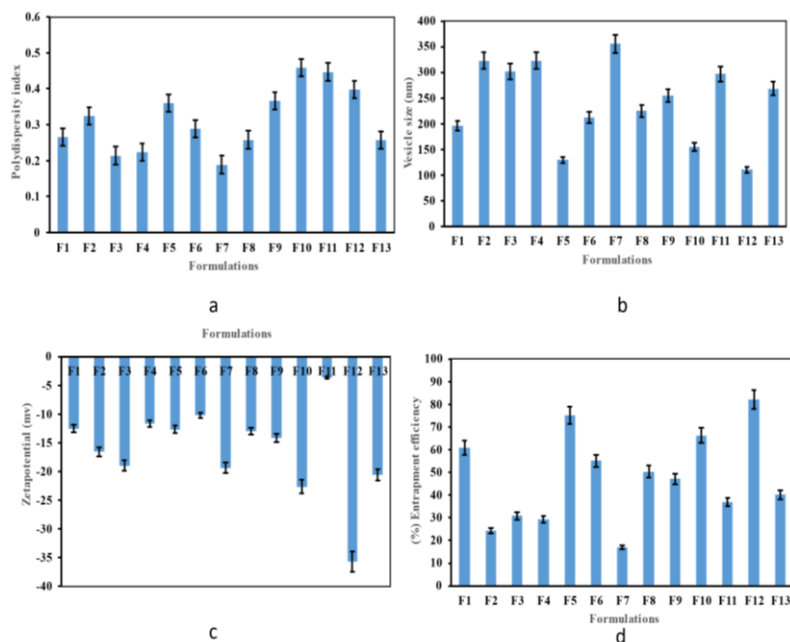
Fig. 7: Bar graph representation of characterization parameters of polydispersity index (a), vesicle size in nm (b), zeta potential in mV (c), and % entrapment efficiency (d) All data showed as mean±SD (n=3); where n is the number of observations

Scanning electron microscopy (SEM)

Morphological research shows that SEM was utilised to better study spherical multilamelar vesicles. SEM micrograph fig. 8 confirms drug-loaded vesicles with smooth and spherical surfaces. The formation of distorted spherical ethosomes may be induced by the hydrophobic effect, which creates vesicles when aqueous (ethanol and water) and non-polar substances (lipids) are kept in contact with one another by external pressure [40].

Powder X-ray diffraction (p-XRD)

Fig. 9a and b show the X-RD patterns of optimised drug-loaded ethosomal gel and pure drug, respectively. Pure-drug exhibited strong peaks at diffraction angles of 6.9°, 8.3°, 9.9°, 19.6°, 20.3°, 21.3°, 25.2°, and 26.4°, indicating the characteristic crystalline pattern. The minimal peak intensity at certain angles in the optimised drug-loaded ethosomal gel decreased gradually, indicating an amorphous shape [41].

***In vitro* release studies of drug-loaded ethosomal gel**

Table 10 shows in vitro drug release data for different types of zolmitriptan-loaded intranasal ethosomal gel formulations. Fig. 10 depicts a nearly identical drug release profile from a gel formulation, including HPMC K100M and poloxamer 407.
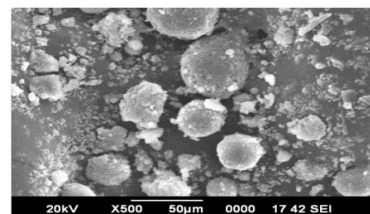

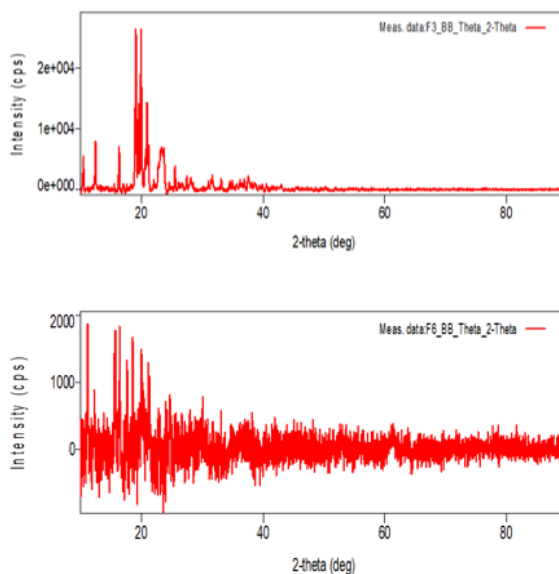**Fig. 8: SEM image of optimized ethosomal F12 formulation**

Fig. 9: P-XRD curve of zolmitriptan pure drug (a) and optimized ethosomal F12 formulation (b)

Table 10: *In vitro* drug release data of different formulations of zolmitriptan-loaded intra-nasal ethosomal gel

| Time (h)	Cumulative drug release (%)												
	F1	F2	F3	F4	F5	F6	F7	F8	F9	F10	F11	F12	F13
0	0	0	0	0	0	0	0	0	0	0	0	0	0
1	15.33	3.04	6.22	5.34	28.22	10.23	1.14	14.40	12.50	20.35	7.28	23.65	9.52
2	35.55	8.24	12.04	10.14	49.54	30.51	4.41	25.24	22.14	45.50	12.44	48.45	18.34
4	40.93	11.21	19.33	14.23	55.89	36.90	8.41	29.13	28.33	50.92	20.61	55.19	24.63
8	48.52	14.65	22.31	18.39	60.52	42.32	11.45	33.24	30.14	58.55	26.74	62.45	27.34
12	54.13	20.81	28.90	24.23	68.15	50.83	14.11	41.22	39.92	64.33	30.01	77.43	34.91
18	60.11	23.22	31.40	26.14	75.82	54.10	17.02	48.19	44.39	70.71	35.11	82.66	38.41
24	64.26	29.65	36.25	30.20	80.22	59.68	20.69	52.82	49.66	75.23	39.22	89.26	42.22
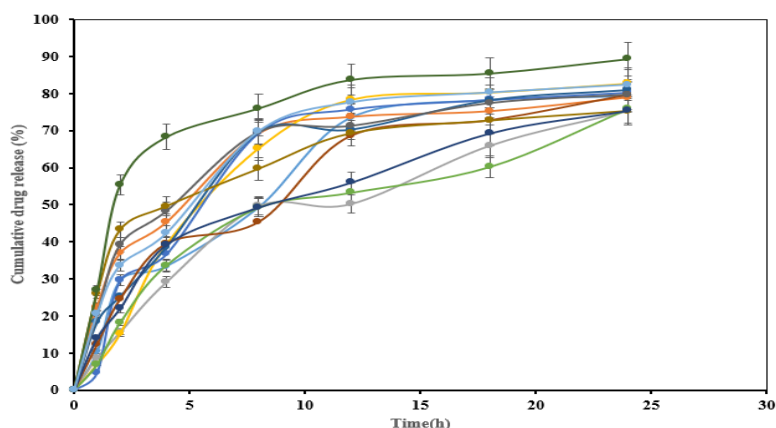
Fig. 10: *In vitro* % drug release graph of different ethosomal formulations of zolmitriptan, All data showed as mean±SD (n=3); where n is the number of observations

Ex vivo skin permeation studies

Fig. 11 depicts the permeability coefficient of a drug-loaded ethosomal gel formulation across the nasal mucosa as a function of the exposure period of contact with mucosal tissues. Permeation experiments on various formulations clearly demonstrate the permeability of the drug-loaded gel through the nasal mucosa [42].
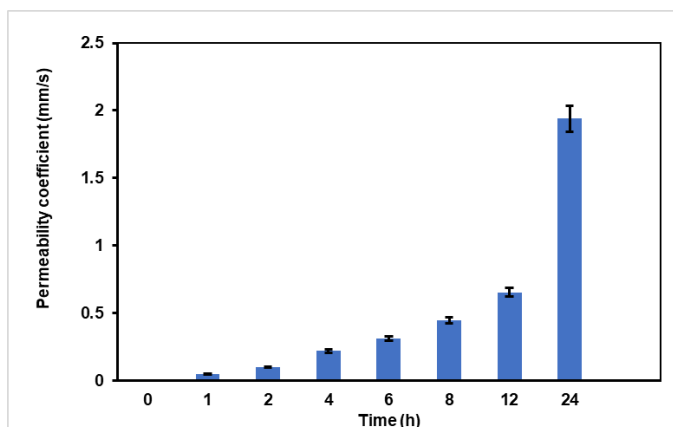

Fig. 11: Permeability coefficient vs time graph of optimized ethosomal F12 formulation, All data showed as mean ± SD (n=3); where n is the number of observations

Table 11: Accelerated stability conditions data of selected parameters for the optimized formulation batch of zolmitriptan-loaded intra-nasal ethosomal gel

Time in (Months)	Cumulative drug release at 24 h (%)	Vesicle size (nm)	Entrapment efficiency (%)
0	89.26	110.23±0.59	82.02±0.75
1	85.256	114.22±0.54	75.363±0.71
2	75.152	122.36±0.51	70.22±0.74
3	73.570	123.55±0.59	69.36±0.77
6	71.223	125.55±0.50	66.55±0.74
*p-value α ≤ (0.05) si*gnificant difference exists	0.061	0.072	0.085

All data showed as mean±SD (n=3); where n is the number of observations

Stability studies

Table 11 displays the p-values obtained using the ANOVA design during the accelerated stability studies. The p-value is greater than 0.05 for all CQAs, indicating that no significant change occurred. As a result, the optimised ethosomal gel of zolmitriptan met the stability criteria because the CQAs did not vary significantly over the study period [43].

CONCLUSION

In this work, the ethosomal gel of zolmitriptan with improved properties was successfully developed by adhering to QbD and DoE ideas. The research confirmed that the use of DoE assisted in identifying and optimizing significant process and material factors to get the required end product quality characteristics. The development of patient-compliant and stable vesicles for improved therapeutic benefits can be facilitated by the use of ethosomalintra nasal gel, as high concentrations of ethanol and soy lecithin were found to be the primary critical material attributes that significantly influence vesicle size, entrapment efficiency, and drug release.

AUTHORS CONTRIBUTIONS

The authors report that this publication is based on the first author's Ph. D. thesis (Nagadivya Nerella), who conducted the preliminary research, collected the data, carried out the work, and produced the entire manuscript. The second author (BAKSHI VASUDHA) was the supervisor, and she revised the text and validated the data for this study. The authors declare no conflicts of interest for this study.

CONFLICT OF INTERESTS

The authors assert that the work presented in this study does not seem to have been influenced by any of their known financial or intimate relationships.

REFERENCES

1. Goadsby PJ, lipton RB, Ferrari MD. Migraine-current understanding and treatment. N Engl J Med. 2002;346(4):257-70. doi: 10.1056/NEJMra010917, PMID 11807151.
2. Palmer KJ, Spencer CM. Zolmitriptan. CNS Drugs. 1997;7(6):468-78. doi: 10.2165/00023210-199707060-00005.
3. Cittadini E, May A, Straube A, Evers S, Bussone G, Goadsby PJ. Effectiveness of intranasal zolmitriptan in acute cluster headache: a randomized, placebo-controlled, double-blind crossover study. Arch Neurol. 2006;63(11):1537-42. doi: 10.1001/archneur.63.11.nct60002, PMID 16966497.
4. Mahakalkar NG, Upadhye KP. Zolmitriptan nasal in-situ gel using sterculia foetida linn gum as natural mucoadhesive polymer. Int J Pharm Sci Rev Res. 2013;22(2):206-13.
5. Dowson AJ, MacGregor EA, Purdy RA, Becker WJ, Green J, Levy SL. Zolmitriptan orally disintegrating tablet is effective in the acute treatment of migraine. Cephalalgia. 2002;22(2):101-6. doi: 10.1046/j.1468-2982.2002.00319.x, PMID 11972576.
6. Belvis R, Pagonabarraga J, Kulisevsky J. Individual triptan selection in migraine attack therapy. Recent Pat CNS Drug Discov. 2009;4(1):70-81. doi: 10.2174/157488909787002555, PMID 19149716.
7. Silberstein SD. Migraine symptoms: results of a survey of self-reported migraineurs. Headache. 1995;35(7):387-96. doi: 10.1111/j.1526-4610.1995.hed3507387.x, PMID 7672955.
8. Elsayed MM, Abdallah OY, Naggar VF, Khalafallah NM. Deformable liposomes and ethosomes: mechanism of enhanced skin delivery. Int J Pharm. 2006;322(1-2):60-6. doi: 10.1016/j.ijpharm.2006.05.027, PMID 16806755.
9. Shelke S, Shahi S, Jalalpure S, Dhamecha D, Shengule S. Formulation and evaluation of thermoreversible mucoadhesive in-situ gel for intranasal delivery of naratriptan hydrochloride. J Drug Deliv Sci Technol. 2015;29:238-44. doi: 10.1016/j.jddst.2015.08.003.
10. Barupal AK, Gupta V, Ramteke S. Preparation and characterization of ethosomes for topical delivery of aceclofenac. Indian J Pharm Sci. 2010;72(5):582-6. doi: 10.4103/0250-474X.78524, PMID 21694989.
11. Sarwa KK, Das PJ, Mazumder B. A nanovesicle topical formulation of Bhut Jolokia (hottest capsicum): a potential anti-arthritic medicine. Expert Opin Drug Deliv. 2014;11(5):661-76. doi: 10.1517/17425247.2014.891581, PMID 24661126.
12. Jain SK, Chourasia MK, Jain AK, Jain RK, Shrivastava AK. Development and characterization of mucoadhesive microspheres bearing salbutamol for nasal delivery. Drug Deliv. 2004;11(2):113-22. doi: 10.1080/10717540490280750, PMID 15200010.
13. Solomon GD, Cady RK, Klapper JA, Earl NL, Saper JR, Ramadan NM. Clinical efficacy and tolerability of 2.5 mg zolmitriptan for the acute treatment of migraine. The 042 clinical trial study group. Neurology. 1997;49(5):1219-25. doi: 10.1212/wnl.49.5.1219, PMID 9371897.
14. MacGregor EA, Brandes J, Eikermann A. Migraine prevalence and treatment patterns: the global migraine and zolmitriptan evaluation survey. Headache. 2003;43(1):19-26. doi: 10.1046/j.1526-4610.2003.03004.x, PMID 12864754.
15. Maheshwari RG, Tekade RK, Sharma PA, Darwhekar G, Tyagi A, Patel RP. Ethosomes and ultra deformable liposomes for transdermal delivery of clotrimazole: a comparative assessment. Saudi Pharm J. 2012;20(2):161-70. doi: 10.1016/j.jsps.2011.10.001, PMID 23960788.
16. Majithiya RJ, Ghosh PK, Umrethia ML, Murthy RS. Thermoreversible-mucoadhesive gel for nasal delivery of sumatriptan. AAPS PharmSciTech. 2006;7(3):67. doi: 10.1208/pt070367, PMID 17025248.
17. Omar SM, AbdAlla FI, Abdelgawad NM. Preparation and optimization of fast-disintegrating tablet containing naratriptan hydrochloride using D-optimal mixture design. AAPS PharmSciTech. 2018;19(6):2472-87. doi: 10.1208/s12249-018-1061-9, PMID 29869307.
18. Shehu IA, Shehu UM, Datta A. Intranasal delivery in managing antibiotic resistance in brain infections. Int J Curr Pharm Sci. 2022;14(2):1-4. doi: 10.22159/ijcpr.2022v14i2.1559.
19. Tepper SJ, Chen S, Reidenbach F, Rapoport AM. Intranasal zolmitriptan for the treatment of acute migraine. Headache. 2013;53Suppl 2:62-71. doi: 10.1111/head.12181, PMID 24024604.
20. El Taweel MM, Aboul Einien MH, Kassem MA, Elkasabgy NA. Intranasal zolmitriptan-loaded bilosomes with extended nasal mucociliary transit time for direct nose-to-brain delivery. Pharmaceutics. 2021;13(11):1828. doi: 10.3390/pharmaceutics13111828, PMID 34834242.
21. Mohamed MI, Abdelbary AA, Kandil SM, Mahmoud TM. Preparation and evaluation of optimized zolmitriptan niosomal emulgel. Drug Dev Ind Pharm. 2019;45(7):1157-67. doi: 10.1080/03639045.2019.1601737, PMID 30919700.
22. Liu C, Fang L. Drug in an adhesive patch of zolmitriptan: formulation and *in vitro /in vivo* correlation. AAPS PharmSciTech. 2015;16(6):1245-53. doi: 10.1208/s12249-015-0303-3, PMID 25771739.
23. Ammar HO, Mohamed MI, Tadros MI, Fouly AA. Transdermal delivery of ondansetron hydrochloride via bilosomal systems: *in vitro*, ex vivo, and *in vivo* characterization studies. AAPS PharmSciTech. 2018;19(5):2276-87. doi: 10.1208/s12249-018-1019-y, PMID 29845503.
24. Misra SK, Pathak K. Nose-to-brain targeting via nanoemulsion: significance and evidence. Colloids Interfaces. 2023;7(1):23. doi: 10.3390/colloids7010023.
25. Wang X, Chi N, Tang X. Preparation of estradiol chitosan nanoparticles for improving nasal absorption and brain targeting. Eur J Pharm Biopharm. 2008;70(3):735-40. doi: 10.1016/j.ejpb.2008.07.005, PMID 18684400.
26. Pathan IB, Jaware BP, Shelke S, Ambekar W. Curcumin loaded ethosomes for transdermal application: formulation, optimization, *in vitro* and *in vivo* study. J Drug Deliv Sci Technol. 2018;44:49-57. doi: 10.1016/j.jddst.2017.11.005.

27. Elsayed MM, Abdallah OY, Naggar VF, Khalafallah NM. Deformable liposomes and ethosomes: mechanism of enhanced skin delivery. Int J Pharm. 2006;322(1-2):60-6. doi: 10.1016/j.ijpharm.2006.05.027, PMID 16806755.

28. Dahlof CG, linde M, Kerekes E. Zolmitriptan nasal spray provides fast relief of migraine symptoms and is preferred by patients: a swedish study of preference in clinical practice. J Headache Pain. 2004;5(4):237-42. doi: 10.1007/s10194-004-0132-3.

29. Hamzah ML, Kassab HJ. Formulation and characterization of intranasal drug delivery of rizatriptan-loaded binary ethosomes gel for brain targeting. Nanotechnol Sci Appl. 2024;17(17):1-19. doi: 10.2147/NSA.S442951, PMID 38249545.

30. Nimisha SK, Singh AK. Formulation and evaluation of sea buckthorn leaf extract loaded ethosomal gel. Asian J Pharm Clin Res. 2015;8(5):316-9.

31. Mohananaidu K, Chatterjee B, Mohamed F, Mahmood S, Hamed Almurisi S. Thermoreversible carbamazepine in situ gel for intranasal delivery: development and *in vitro*, ex vivo evaluation. AAPS PharmSciTech. 2022;23(8):288. doi: 10.1208/s12249-022-02439-x, PMID 36271212.

32. Dayan N, Touitou E. Carriers for skin delivery of trihexyphenidyl HCl: ethosomes vs. liposomes. Biomaterials. 2000;21(18):1879-85. doi: 10.1016/s0142-9612(00)00063-6, PMID 10919691.

33. Bhalerao AV, lonkar SL, Deshkar SS. Nasal mucoadhesive in situ gel of ondansetron hydrochloride. Indian J Pharm Sci. 2009;71:711-3.

34. El Taweel MM, Aboul-Einien MH, Kassem MA, Elkasabgy NA. Intranasal zolmitriptan-loaded bilosomes with extended nasal mucociliary transit time for direct nose-to-brain delivery. Pharmaceutics. 2021;13(11):1828. doi: 10.3390/pharmaceutics13111828, PMID 34834242.

35. Thakkar H, Vaghela D, Patel BP. Brain targeted intranasal in-situ gelling spray of paroxetine: formulation, characterization and *in vivo* evaluation. J Drug Deliv Sci Technol. 2021;62:102317. doi: 10.1016/j.jddst.2020.102317.

36. Shelke S, Shahi S, Jalalpure S, Dhamecha D. Poloxamer 407-based intranasal thermoreversible gel of zolmitriptan-loaded nanoethosomes: formulation, optimization, evaluation and permeation studies. J Liposome Res. 2016 Dec;26(4):313-23. doi: 10.3109/08982104.2015.1132232, PMID 26758957.

37. Grace XF, KS, SS. Development of terminalia chebula-loaded ethosomal gel for transdermal drug delivery. Asian J Pharm Clin Res. 2018;11(12):380-3. doi: 10.22159/ajpcr.2018.v11i12.20764.

38. Shin BK, Baek EJ, Choi SG, Davaa E, Nho YC, Lim YM. Preparation and irradiation of pluronic F127-based thermoreversible and mucoadhesive hydrogel for local delivery of naproxen. Drug Dev Ind Pharm. 2013;39(12):1874-80. doi: 10.3109/03639045.2012.665925, PMID 22409199.

39. Deleu D, Hanssens Y. Current and emerging second-generation triptans in acute migraine therapy: a comparative review. J Clin Pharmacol. 2000;40(7):687-700. doi: 10.1177/00912700022009431, PMID 10883409.

40. Ghose D, Patra CN, Ravi Kumar BV, Swain S, Jena BR, Choudhury P. QbD-based formulation optimization and characterization of polymeric nanoparticles of cinacalcet hydrochloride with improved biopharmaceutical attributes. Turk J Pharm Sci. 2021 Sep 1;18(4):452-64. doi: 10.4274/tjps.galenos.2020.08522, PMID 34496552.

41. Beg S, Swain S, Singh HP, Patra ChN, Rao ME. Development, optimization, and characterization of solid self-nanoemulsifying drug delivery systems of valsartan using porous carriers. AAPS PharmSciTech. 2012;13(4):1416-27. doi: 10.1208/s12249-012-9865-5, PMID 23070560.

42. Parhi R, Swain S. Transdermal evaporation drug delivery system: concept to commercial products. Adv Pharm Bull. 2018;8(4):535-50. doi: 10.15171/apb.2018.063, PMID 30607327.

43. Jena BR, Panda SP, Kulandaivelu U, Alavala RR, Rao GS, Swain S. AQbD driven development of an RP-HPLC method for the quantitation of abiraterone acetate for its pharmaceutical formulations in the presence of degradants. Turk J Pharm Sci. 2021;18(6):718-29. doi: 10.4274/tjps.galenos.2021.74150, PMID 34978401.